Copper microRNAs modulate the formation of giant feeding cells induced by the root knot nematode Meloidogyne incognita in Arabidopsis thaliana

Yara Noureddine, Joffrey Mejias, Martine da Rocha, Sébastien Thomine, Michaël Quentin, Pierre Abad, Bruno Favery, Stéphanie Jaubert-Possamai

Copper microRNAs modulate the formation of giant feeding cells induced by the root knot nematode *Meloidogyne incognita* in *Arabidopsis thaliana*

Yara Noureddine[1], Joffrey Mejias[1], Martine da Rocha[1], Sébastien Thomine[2], Michaël Quentin[1], Pierre Abad[1], Bruno Favery[1], and Stéphanie Jaubert-Possamai[1*]

1 INRAE, Université Côte d'Azur, CNRS, ISA, Sophia Antipolis, F-06903, France

2 Institute for Integrative Biology of the Cell (I2BC), UMR9198 CNRS/CEA/Univ. Paris Sud, Université Paris-Saclay, Gif-sur-Yvette, France.

Corresponding author: stephanie.jaubert@inrae.fr

Word Count. 5050

Introduction: 1,127 words

Materials and Methods: 872 words

Results: 1842 words

Discussion: 1222 words

Acknowledgements: 147 words

Number of Tables: 1

Number of figures: 5 (all in colors)

Supporting information: 10 figures and 10 tables.

Heading

Arabidopsis copper microRNAs modulate the development of feeding site induced by root knot nematodes.

Twitter :

@stephejaubert

@noureddine_yara

@brunofavery

ORCID :

Stéphanie Jaubert-Possamai : https://orcid.org/0000-0002-3518-727X
Yara Noureddine : https://orcid.org/0000-0002-6875-5835
Joffrey Mejias : https://orcid.org/0000-0001-7663-0314
Martine da Rocha : https://orcid.org/0000-0003-0959-2295
Sébastien Thomine : https://orcid.org/0000-0003-0045-1701
Michaël Quentin : https://orcid.org/0000-0002-8030-1203
Pierre Abad : https://orcid.org/0000-0003-0062-3876
Bruno Favery : https://orcid.org/0000-0003-3323-1852

Summary (161 words)

- Root-knot nematodes (RKN) are root endoparasites that induce the dedifferentiation of a few root cells and the reprogramming of their gene expression to generate giant hypermetabolic feeding cells.
- We identified two microRNA families, miR408 and miR398, as upregulated in *Arabidopsis thaliana* and *Solanum lycopersicum* roots infected by root-knot nematodes. In plants, the expression of these two conserved microRNA families is known to be activated by the SPL7 transcription factor in response to copper starvation.
- By combining functional approaches, we deciphered the network involving these microRNAs, their regulator and their targets. *MIR408* expression was located within nematode-induced feeding cells like its regulator *SPL7* and was regulated by copper. Moreover, infection assays with *mir408* and *spl7* KO mutants or lines expressing targets rendered resistant to cleavage by miR398 demonstrated the essential role of the *SPL7*/*MIR408*/*MIR398* module in the formation of giant feeding cells.
- Our findings reveal how perturbation of plant copper homeostasis, *via* the *SPL7*/*MIR408*/*MIR398* module, modulates the development of nematode-induced feeding cells.

Key words: root-knot nematodes, microRNAs, copper, signaling, *Arabidopsis*

Introduction

MicroRNAs are small non-coding RNAs that regulate the expression of protein-coding genes, mostly at the post-transcriptional level, in plants. They are major post-transcriptional regulators of gene expression in various biological processes, including plant development (Li and Zhang, 2016), responses to abiotic stresses (Barciszewska-Pacak *et al*., 2015), hormone signalling (Curaba et al., 2014), and responses to pathogens or symbiotic micro-organisms (Hoang *et al*., 2020; Weiberg and Jin, 2015). MicroRNAs and short interfering RNAs (siRNAs) were recently shown to play a key role in plant-pathogen crosstalk through trans-kingdom RNAi processes (Weiberg *et al*., 2013; Cai et al., 2018; Dunker *et al*., 2020). MicroRNAs are produced by the cleavage of long double-stranded RNA precursors by the DICER RNAse, generating 20-22 nucleotides miRNA duplexes composed of a mature (5P) and a complementary (3P) strand. One of the two strands is then incorporated into the RNA-induced silencing complex (RISC) to guide the major RISC protein, ARGONAUTE1 (AGO1), to the targeted messenger RNA (mRNA) on the basis of sequence complementarity. The hybridization of AGO1-bound miRNAs to their targets induces predominantly targeted mRNA degradation in plants, but it may also lead to an inhibition of mRNA translation (Axtell, 2013).

The miR408 and miR398 microRNA families are conserved so-called "copper microRNAs", due to their function in the plant response to copper deficiency (Zhang *et al*., 2015; Yamasaki *et al*., 2007). Copper is an essential nutrient for plants, due to its function as a cofactor for many proteins. Copper proteins are involved in electron transport chains or function as enzymes in redox reactions. In plants, copper is involved in respiration, photosynthesis, ethylene perception, the metabolism of reactive oxygen species and cell wall remodelling (reviewed in Burkhead *et al*., 2009). Copper microRNAs accumulate in response to copper deficiency and their synthesis is repressed when copper concentrations are sufficiently high (Yamasaki *et al*., 2009). The underlying mechanism has been described in *Arabidopsis thaliana*, in which the regulation of *MIR408, MIR398B* and *MIR398C* by copper levels was shown to be mediated by the SQUAMOSA PROMOTER-BINDING PROTEIN-LIKE7 (SPL7) transcription factor (Yamasaki *et al*., 2009). The *A. thaliana* genome contains a single copy of *MIR408,* and three *MIR398* genes: *MIR398A, -B and -C*. At high copper concentrations, the DNA-binding activity of the SPL7 transcription factor is repressed, preventing the induction of transcription for downstream genes, such as *MIR408* or *MIR398B* and *MIR398C,* but not *MIR398A* (Sommer *et al*., 2011; Yamasaki *et al*., 2009). In the presence of low concentrations of copper, SPL7 activates the expression of copper-responsive microRNAs that target and repress the expression

of genes encoding copper-binding proteins. These proteins are replaced by proteins that do not bind copper, to save copper resources for the functions for which this element is essential, such as photosynthesis (reviewed in Burkhead *et al*., 2009). For example, the mRNA for the cytosolic COPPER/ZINC (Cu-Zn) SUPEROXIDE DISMUTASE, CSD1, which can be replaced by an iron (Fe)-dependent SOD, is targeted by the copper microRNA miR398. In addition to their regulation as a function of copper levels through the activity of SPL7, *MIR408* and the *MIR398* family are also regulated by several environmental cues and abiotic stresses, such as light, which regulates *MIR408* activity through the ELONGATED HYPOCOTYL5 (HY5) or PHYTOCHROME INTERACTING FACTOR1 (PIF1) transcription factors in *A. thaliana* (Jiang *et al*., 2021), and salinity, oxidative and cold stresses, which have been shown to induce *MIR408* in *A. thaliana* (Ma *et al*., 2015), or cadmium treatment in *Brassica napus* (Fu *et al*., 2019). The miR408 and miR398 families have been widely analysed in plant responses to abiotic stresses, but little is known of their role in plant responses to biotic stresses. In sweet potato, *MIR408* has been associated with plant defences, as it is repressed by jasmonic acid (JA) and wounding, and miR408-overexpressing plants have attenuated resistance to insect feeding (Kuo *et al*., 2019). Moreover, miR398 has been shown to regulate cell death in response to the causal agent of barley powdery mildew, *Blumeria graminis (Xu et al.*, 2014).

Root-knot nematodes (RKN) of the genus *Meloidogyne* are obligatory sedentary plant parasites capable of infesting more than 5,000 plant species (Abad and Williamson, 2010; Blok *et al*., 2008). The RKN larvae penetrate the roots, in which they induce the de-differentiation of five to seven parenchyma root cells and their reprogramming into the multinucleate, hypertrophied feeding cells that form the feeding site. These metabolically overactive feeding cells provide the nutrients required for RKN development (Favery *et al*., 2020). During the dedifferentiation of vascular cells and their conversion into 'giant' feeding cells, the cells surrounding the feeding site begin to divide again. The growth of the feeding cells and the division of the surrounding cells lead to a root swelling known as a gall. The feeding cell induction occurs in the first three days after root infection. Feeding cell formation can be split into two phases. Firstly, the cells undergo successive nuclear divisions coupled with cell expansion until ten days post infection (dpi) in *A. thaliana* (Caillaud *et al.*, 2008). In the second phase, from 10 to 21 dpi, the successive nuclear divisions stop and the nuclei of the feeding cells undergo extensive endoreduplication (Wiggers *et al*., 1990; de Almeida Engler and Gheysen, 2013). The dedifferentiation of vascular cells and their conversion into giant cells result from an extensive reprogramming of gene expression in root cells, in response to RKN signals. In *A. thaliana*, the expression of

approximately 10% of protein-coding genes is modified in galls induced by RKN (Cabrera *et al*., 2014; Yamaguchi *et al*., 2017; Jammes *et al*., 2005; reviewed in Escobar *et al*., 2011). The sequencing of small RNAs identified 24 mature microRNAs differentially expressed (DE) between *A. thaliana* galls induced by *M. incognita* and uninfected roots at 7 and 14 dpi and 62 microRNAs DE at 3 dpi (Medina *et al*., 2017; Cabrera *et al*. 2015). The miR408 and miR398 families of copper-responsive microRNAs were found to be upregulated in galls at 7 and/or 14 dpi.

In this article, we showed a conserved upregulation of these two microRNA families in *Arabidopsis* and tomato galls. Moreover, we found that the upregulation of *MIR408* in response to RKN was required for successful infection. Our findings highlighted a strong activity of the *MIR408* promoter (*pMIR408*) in early galls that is i) driven by the modulation of environmental copper levels, ii) **is localised in the same gall tissue than the strong *SPL7* expression**. Moreover, we also demonstrated that this transcription factor helps to promote giant cell development. In addition, we showed that the silencing of *CSD1* and *BLUE COPPER BINDING PROTEIN* (*BCBP*) transcripts by miR398 is involved in gall development. Finally, the watering of *Arabidopsis* with copper sulphate solutions at concentrations below the toxicity thresholds for nematode and plant development greatly decreased the RKN infection and impaired feeding cell development.

Material and Methods

Biological material, growth conditions and nematode inoculation

Seeds of *A. thaliana* Col0 and mutants *mir408-1* (SALK_038860), *mir408-2* (SALK_121013.28.25.n), *spl7* (SALK_093849), *mcsd1* and *mbcbp* (Beauclair *et al*., 2010), *pmiR408::GUS* (Zhang *et al*., 2013) and *pSPL7::GUS* (Yamasaki *et al*., 2009) were surface-sterilised and sown on Gamborg B5 medium agar plates (0.5 x Gamborg, 1% sucrose, 0.8% agar, pH 6.4). The plates were incubated at 4°C for two days, then transferred to a growth chamber (20°C with an 8 h light/ 16 h darkness cycle). *M. incognita* strain "Morelos" was multiplied on tomato plants in a growth chamber (25°C, 16 h light/8 h darkness). For the RKN infection of plants in soil, two-week-old plantlets grown *in vitro* were transferred to a mixture of 50% sand (Biot B5)/50% soil in a growth chamber (21°C, 8 h light/16 h darkness). For studies of the effect of copper on gall development on plants *in vitro*, *Arabidopsis* plantlets were sown and cultured *in vitro,* as described above, on Gamborg B5 medium supplemented with 50 µM $CuSO_4$.

Root knot nematode infection assay

For nematode infections *in vitro*, second-stage juveniles (J2s) were surface-sterilised with $HgCl_2$ (0.01%) and streptomycin (0.7%), as described by Caillaud and Favery (2016). We inoculated each 25-day-old seedling grown individually *in vitro* with 200 sterilised J2s resuspended in Phytagel (5%). Infection assays were performed on *Arabidopsis* mutants and a wild-type ecotype in soil. We inoculated 20 to 30 two-month-old plantlets with 150 J2s per plant and incubated them in a growth chamber (21°C, 8 h light/16 h darkness). Seven weeks after infection, the roots were collected, washed in tap water and stained with eosin (0.5 %). Stained roots were weighed and galls and egg masses were counted on each root under a binocular microscope. Mann and Whitney tests (2.5%) were performed to determine the significance of the observed differences in the numbers of egg masses and galls per root.

Small RNA sequencing from galls and uninfected tomato roots

Biological material, RNA extraction, small RNA and RNA sequencing, read mapping and statistical analysis are presented as supporting informations (Method S1-S6).

BABB clearing

Feeding site development was evaluated by the BABB clearing method described by Cabrera *et al*., (2018). Briefly, the area occupied by the giant cells was measured on galls collected seven weeks post infection, cleared in benzyl alcohol/benzyl benzoate (BABB) and examined under an inverted confocal microscope (model LSM 880; Zeiss). Zeiss ZEN software was used to measure the area occupied by the giant cells in each gall, on two biological replicates. Data were analysed in Mann and Whitney tests.

Copper treatment

M. incognita eggs were collected as previously described (Caillaud and Favery, 2016) and placed on a 10 µm-mesh sieve for hatching in tap water. Free-living J2s were collected from the water with a 0.5 µm-mesh sieve. We evaluated the toxicity of copper to J2s by incubating freshly hatched J2s in solutions of copper sulphate of various concentrations for 24 hours. The numbers of living or dead J2s were then determined by counting under a binocular microscope. We investigated the effects of copper on plant-nematode interactions in *Arabidopsis* Col0 grown in soil. *Arabidopsis* Col0 plantlets were prepared and inoculated as previously described for in-soil infection. Half the plants were watered with 50 µM $CuSO_4$ two days after inoculation with J2s and then once per week for the next seven weeks. Control Col0 plants were watered with tap water in place of copper sulphate solution, at the same frequency. Seven weeks after

inoculation, the plants were collected, their roots were washed and weighed, and the numbers of galls and egg masses on the roots were counted, as described above.

Studies of promoter-GUS fusion gene expression

We localised the promoter activity of *MIR408* and *SPL7* in *A. thaliana* lines expressing various fusions of the *GUS* reporter gene to promoters from these genes. We inoculated 21-day-old seedlings in soil and *in vitro,* as described above. We collected inoculated roots and washed them in water, 3, 7, 14 and 21 dpi. GUS staining was performed as previously described (Favery *et al.*, 1998), and the roots were observed under a Zeiss Axioplan 2 microscope. Stained galls were dissected, fixed by incubation in 1% glutaraldehyde and 4% formaldehyde in 50 mM sodium phosphate buffer pH 7.2, dehydrated, and embedded in Technovit 7100 (Heraeus Kulzer, Wehrheim, Germany), according to the manufacturer's instructions. Sections were cut and mounted in DPX (VWR International Ltd, Poole, UK), and observed under a Zeiss Axioplan 2 microscope (Zeiss, Jena, Germany).

Bioinformatic analysis

We used psRNA target with default parameters for the prediction of miR408 targets (Dai, Zhuang and Zhao 2018).

Quantitative PCR

Total RNA was extracted from galls and uninfected roots produced in soil with the miRNeasy kit (QIAGEN) according to the manufacturer's instruction. 500ng of total RNA were subjected to reverse transcription with the Superscript IV reverse transcriptase (Invitrogen). qPCR analyses were performed as described by Nguyen *et al*. (2018). We performed qPCR on triplicate samples of each cDNA from three independent biological replicates. *OXA1* (*At5g62050*) and *UBP22* (*AT5G10790*) were used for the normalization of qRT-PCR data. Quantifications and statistical analyses were performed with SATqPCR (Rancurel *et al*., 2019), and the results are expressed as normalized relative quantities. Primers used to amplify the premiRNAs and the transcripts are listed in Table S1.

NBT staining of galls

Biological material, and NBT staining of galls are presented as supporting information (Method S7).

Results

MIR408 is induced in galls and its expression is driven by modulation of copper level

Previous sequencing analyses of microRNAs expressed in *Arabidopsis* galls induced by *M. incognita* revealed an upregulation of mature miR408 in *Arabidopsis* galls at 7 and 14 dpi, whereas miR398b/c was specifically upregulated in galls at 14 dpi. None of these microRNAs were shown as DE in galls at 3 dpi produced from young *in vitro* plantlets (Cabrera *et al*. 2016). Sequencing of small RNAs from uninfected roots and galls of *Solanum lycopersicum* showed that these two microRNA families were also upregulated in tomato galls at 7 and 14 dpi (Table 1 and Table S2). Therefore, these microRNAs are among the very few conserved microRNAs which expression profile is conserved in *Arabidopsis* and tomato galls. We investigated the induction of *MIR408* in response to nematode infection, by inoculating plants expressing pMIR408::GUS (Zhang and Li, 2013) grown *in vitro* on Gamborg B5 with *M. incognita* J2s. We observed a strong GUS signal in developing galls at 3 and 7 dpi (Fig. 1a-b). This signal had decreased in intensity by 14 dpi (Fig. 1c) and disappeared completely from fully developed galls at 21 and 28 dpi (Fig. S1). On gall sections, the GUS signal was localised in the giant feeding cells and neighbouring cells, at the 3 dpi, 7 dpi and 14 dpi time points (Fig. 1d-f). Overexpression of *MIR408* at 7 dpi was confirmed by qPCR analysis of level of premiR408 in galls at 7 and 14 dpi (Fig S2). The discrepancy between mature miR408 and premiR408 level in galls at 14 dpi may be explained by the delay between transcription of premiRNA and its processing into mature microRNA by Dicer as it has been previously described (Thompson *et al.*, 2006; Hutvagner *et al.*, 2001; Schulman *et al.*, 2005). MiR408 is known as a copper microRNA. To investigate if copper modulation regulates *MIR408* expression in galls, *pMIR408::GUS* activity was followed in plants grown *in vitro* with a high copper concentration (Gamborg B5 plus 5 µM $CuSO_4$). By contrast to plants grown in Gamborg B5, in plants grown in the presence of high copper concentrations, the GUS signal was much weaker in galls at 3 and 7 dpi (Fig. 1g-h and 1j-k), and undetectable in galls at 14 dpi (Fig. 1i and 1l). The repression of *MIR408* expression in galls by high copper concentrations indicates that *MIR408* expression within *Arabidopsis* galls is regulated by modulation of copper levels.

The copper microRNA miR408 is crucial for the *Arabidopsis-Meloidogyne* interaction

We investigated the role of miR408 in gall development using two previously described *Arabidopsis* knockout (KO) mutant lines: *mir408-1* and *mir408-2* (Maunoury and Vaucheret,

2011). The KO lines and corresponding wild-type plants were inoculated with *M. incognita* J2s and their susceptibility was quantified by counting the galls and egg masses produced by adult females at the root surface. The two KO lines for *MIR408* had 40 to 50% fewer galls and egg masses than the wild type (p<0.05; Fig. 2 and Table S3). The roots of these KO lines were of similar weight and global architecture to those of wild-type plants (Fig. S2 and Table S3). We then investigated the effect of the *MIR408* mutation on feeding site development, by comparing the area of feeding cells within galls collected from KO and wild-type plants (Fig. 2a-c and Table S3). Both KO mutants had a significantly smaller feeding site area than the wild type. Overall, these results demonstrate that *MIR408* helps to promote feeding cell development in the *Arabidopsis*-nematode interaction, and that the lower susceptibility of the *miR408* KO lines is due to defects of feeding site development.

We investigated the targeted transcripts by which miR408 modulates feeding cell development in galls. The psRNA target algorithm (Dai *et al*., 2018) predicted 101 genes as putative targets of miR408 in *Arabidopsis* (Table S4a). The expression profiles of these genes in galls at 7 dpi and 14 dpi were obtained from previous transcriptome analyses (Jammes *et al*. 2005). Only seven of the 101 putative targets were differentially expressed in galls at 7 and/or 14 dpi, and only two putative targets were repressed: a transcript encoding a copper-binding protein, UCLACYANIN2 (*UCC2*, *At2g44790*), which is known to be cleaved by the RNA INDUCED SILENCING COMPLEX (RISC) guided by miR408 in senescing leaves and siliques (Thatcher *et al*., 2015), and a transcript encoding a PHOSPHATASE 2G (*PP2CG1*, *At2g33700*) (Table S4b). The repression of these two genes was confirmed in galls at 14 dpi by qPCR (Fig. S3 and Table S5) supporting that mature miR408 induced the cleavage of these two targets at this time point.

SPL7 is an activator of *MIR408* transcription in galls

The regulation of *MIR408* by modulation of copper levels has been shown to be mediated by the SPL7 transcription factor (Zhang *et al*., 2014; Bernal *et al*., 2012). Transcriptome analyses from *Arabidopsis* galls showed that *SPL7* was expressed in galls at 7, 14 and 21 dpi (Jammes *et al*., 2005). We further investigated the expression of *SPL7* within galls, by inoculating a *pSPL7::GUS Arabidopsis* line (Araki *et al*., 2018) with *M. incognita* in the presence of a normal copper concentration. *SPL7* promoter activity was observed within the gall from 3 to 14 dpi, with lower levels at 14 dpi (Fig. 3a-c). As observed for *pMIR408::GUS*, sections of

pSPL7::GUS galls revealed a GUS signal in the giant feeding cells and neighbouring cells (Fig. 3d). We investigated the putative function of *SPL7* in plant responses to RKN, by inoculating the *Arabidopsis spl7* KO mutant described by Zhang *et al*. (2014) with *M. incognita* J2s. *SPL7* knockout led to the production of smaller numbers of galls and egg masses per plant than were observed for the wild-type (Fig. 3e-f and Table S6). This knockout had no effect on root weight (Fig. S4 and Table S6). Measurements of the area of the feeding site within galls revealed defects of feeding site formation in the *spl7* mutants, resulting in smaller giant cells than were observed in wild-type plants (Fig. 3g and Table S6). Overall, these results demonstrate the requirement of miR408 and SPL7 for the proper development of giant cells. The upregulation of mature miR408 observed in galls suggests an induction of *MIR408* expression driven by SPL7 due to a decrease in copper availability within the gall.

micro398, a second copper-responsive microRNA family involved in the *Arabidopsis-Meloidogyne* interaction

MiR408 is not the only copper-responsive microRNA reported differentially expressed in galls. The expression of *MIR398B* and *MIR398C,* from the conserved miR398 family, has also been shown to be induced in response to copper deficiency, via SPL7 activity (Araki *et al*., 2018). We previously described an induction of the mature miR398b and miR398c in *Arabidopsis* galls at 14 dpi by sequencing (Medina *et al*., 2017). However, quantification of the precursors by qPCR did not confirm the induction of the mature miR398s (Fig S5 and Table S7). Three targets of the miR398 family have been biologically validated: the *At1g08830* and *At2g28190* transcripts encoding two copper superoxide dismutases, *CSD1* and *CSD2,* respectively, and the *At5g20230* transcript encoding the blue copper binding protein (BCBP), identified as a non-canonical target of miR398 (Brousse *et al*., 2014). Previous analyses of *Arabidopsis* gall transcriptome showed a repression of *CSD1* at 7 dpi and of *BCBP* at 7 and 14 dpi while *CSD2* was not differentially expressed (Jammes *et al*. 2005). qPCR did not confirm the repression of *CSD1* and *CSD2* and showed a repression of *BCBP* at 7 dpi but with a pvalue of 0.07 (Fig. S5 and Table S7). Despite the lack of confirmation of sequencing and microarray results by qPCR, we investigated the role of miR398 further, by infecting *Arabidopsis* lines expressing modified versions of *CSD1* (*mcsd1*) or *BCBP (mbcbp)* mRNAs rendered resistant to cleavage by miR398 (Brousse *et al*., 2014; Beauclair *et al*., 2010). The target mRNA levels is therefore artificially increased in these plants. The prevention of *CSD1* transcript cleavage by miR398 had no effect on root weight (Fig. S6), but led to lower levels of nematode infection, with the mutant having less galls and egg masses than the wild type (Fig. 4 and Table S8). The *mbcbp* line also had

fewer egg masses than the wild-type (Fig. 4 and Table S8). No defect of feeding cell formation, such as slower feeding cell growth, was observed in either of these lines (Fig. 4 and Table S8). The specific decrease in egg mass production by females provides evidence for a role for miR398 in the functionality of feeding cells, although the mutations in the *mcsd1* and *mbcbp* lines did not affect feeding site size (Fig. 4). These findings demonstrate that the cleavage of *CSD1* and *BCBP* transcripts by the RISC guided by miR398 helps to promote parasitism.

Modulation of copper levels is essential for plant-RKN interaction

To study further the effect of copper on nematode infection, we analysed the direct effects of copper on nematode survival and gall development. Free-living *M. incognita* J2s were incubated in several concentrations of copper sulphate (50 µM to 2 mM) used in previous studies assessing the effect of copper on plant development (Schulten *et al*., 2019). As a negative control, J2s were incubated in tap water. Living J2 counts after 24 hours in the copper sulphate solution showed that copper was non-toxic at a concentration of 50 µM (Fig. S7 and Table S9). By contrast, toxic effects were observed for all other concentrations tested (0.5 mM, 1 mM and 2 mM). We then analysed the effect of copper on gall formation in Col0 and *pMIR408::GUS* plants grown in soil watered with 50 µM $CuSO_4$. We also minimised J2s exposure to copper in the soil, by beginning to water plants 50 µM $CuSO_4$ two days after inoculation, after the J2s had already penetrated the roots. Watering with 50 µM $CuSO_4$ repressed pMIR408 activity in uninfected roots and in galls as it can be observed by the reduction of the GUS signal (Fig. S8) confirming the effects of such treatment in galls. Watering with 50 µM $CuSO_4$ had no visible effect on root weight and architecture (Fig. S9 and Table S10), but it resulted in a strong and significant decrease in the number of galls and egg masses relative to control plants watered with tap water (Fig. 5). Copper is involved in many processes in plants like the production of reactive oxygen species (ROS). Watering plants with CuSO4 may therefore have additional effects in addition to the repression of the *pMIR408* activity. The effect of watering with $CuSO_4$ on ROS production during the nematode infection was analysed. The 0^{2-} accumulation was followed by Nitro Blue Tetrazolium (NBT) staining of galls collected 14 dpi from plants watered with tap water or with 50 µM $CuSO_4$. NBT staining showed the same localisation and intensity signal in galls regardless the watering condition. A strong 0^{2-} accumulation can be observed in cells surrounding the feeding site when the giant feeding cells showed no signal (Fig. S10). Altogether, these results demonstrate that perturbation of plant copper homeostasis modulates miR408 production in galls and interferes with the plant-RKN interaction.

Discussion

RKN induce the formation of similar giant feeding cells in thousands of plant species. The conservation of the ontogeny and phenotype of nematode-induced feeding cells between species, strongly suggests that the plant molecular mechanisms manipulated by RKN are widely conserved across the plant kingdom. Previous transcriptome analyses on various plant species have shown that the development of galls in roots infected by RKN is associated with a massive reprogramming of gene expression (reviewed in Escobar *et al*., 2011). MicroRNAs are small non-coding RNAs that regulate gene expression at the post-transcriptional level, and some microRNA families, such as the miR156 and miR167 families, are widely conserved in plants (Chavez Montes *et al*., 2014). The role for microRNAs in controlling gene expression during the formation of galls was recently reported in *Arabidopsis* (reviewed in Jaubert-Possamai *et al*., 2019), for the conserved microRNAs miR390, miR172 and miR159 (Cabrera *et al*. 2016; Diaz-Manzano *et al*. 2018; Medina *et al*., 2017).

miR408 and miR398: two copper-responsive microRNA families activated in galls induced by *M. incognita*

Sequencing of small RNAs showed that mature miR408 and miR398b/c microRNAs accumulated in galls at 7 and/or 14 dpi, compared to uninfected roots, in both *A. thaliana* (Medina *et al*., 2017) and *S. lycopersicum* . A combination of *in silico* predictions of the transcripts targeted by miR408 and transcriptional analyses of galls and uninfected roots identified the *UCLACYANIN-2* (*UCC2*) and the *PHOSPHATASE* (*PP2CG*) genes as two putative targets of miR408 downregulated in galls . The cleavage of *UCC2* transcripts by miR408 has been biologically validated in *Arabidopsis* and rice (Thatcher *et al*., 2015; Zhang *et al*., 2017). Moreover, several targets of miR398 have been biologically validated, including the cytosolic *CSD1* and chloroplastic *CSD2*, and the non-canonical target *BCBP* (Beauclair *et al*., 2010; Brousse *et al*., 2014). Our analysis, thus, identified several biologically validated and conserved targets that may be considered robust candidates for mediating the functions of miR398b/c and miR408 in galls.

The inactivation of miR408 in *Arabidopsis* T-DNA mutant lines, or of miR398b/c function in transgenic plants expressing mutated *CSD1* or *BCBP* resistant to miR398 cleavage, led to decreases in both the parameters used to assess parasitic success (the number of galls and the number of females producing egg masses per root). The smaller number of galls in the mutant lines demonstrates that miR398 family and miR408 promote infection in the early plant

response to RKN. Moreover, the smaller feeding sites observed in the two *miR408* KO lines and the *spl7* mutant demonstrate that this miR408 and SPL7 promote the development of the giant cells, which are essential for nematode growth and development. Females are unable to develop normally if the feeding cells are too small, as already reported in some *Arabidopsis* mutants, such as lines with a knockout of *PHYTOSULFOKINE RECEPTOR1 (PSKR1)* (Rodiuc *et al*., 2016). Only a few genes and plant functions have been demonstrated to be essential for the formation of giant feeding cells (Favery *et al.,* 2020). In the absence of changes in giant cell size in the *mcsd1* and *mbcbp* mutants, we hypothesise that the miR398-regulated *CSD1* and *BCBP* genes may play a role in giant cell functioning, potentially in reactive oxygen species (ROS)-related redox regulation and signalling (Zhao *et al*., 2020). Further studies will be required to determine their precise roles in the plant-RKN interaction.

SPL7 is a regulator of miR408 and miR398 in galls

In *A. thaliana,* it has been shown that *MIR408*, *MIR398B* and *MIR398C* are activated by the same transcription factor, SPL7, the activity of which is dependent on copper levels (Yamasaki *et al*., 2009; Araki *et al*., 2018). We confirmed the activity of the *SPL7* promoter and *MIR408* in feeding cells and neighbouring cells. The co-expression of *SPL7* and *MIR408* within developing galls, and the similar nematode infection phenotype, with feeding site formation defects, strongly suggest that *SPL7* is responsible for activating *MIR408* transcription in galls, as already reported in leaves and the root vasculature (Yamasaki *et al*., 2009; Araki *et al*., 2018). We therefore hypothesised that the expression of *MIR408* and *MIR398B* and -*C* is activated by the SPL7 transcription factor in response to a decrease in copper concentration within galls. Other transcription factors, such as HY5 and PIF1, which are known to regulate the expression of *MIR408* in response to light stress (Zhang *et al*., 2014; Jiang *et al*., 2021), are expressed in galls and could also play a role in the regulation of *MIR408* expression. The strong repression of *MIR408* by excess copper observed in galls suggests that *MIR408* upregulation in galls is predominantly driven by copper and SPL7. However, we can't exclude that nematode effectors may also influence directly the expression of *MIR408* and *MIR398* in addition to the regulation by copper modulation. Further analyses are now required to understand how these microRNAs are induced in response to nematode infection.

Modulation of copper levels, a key conserved factor for gall formation

Infection assays on *A. thaliana* plants watered with a copper sulphate solution at a concentration non-toxic for plants and nematodes, showed a strong decreased RKN infection rates and resulted in defective feeding site formation. Together with the upregulation in galls of two microRNA families known to be induced by copper deficiency, the miR408 and miR398 families, and the regulation of *MIR408* expression by copper, this finding suggests that copper content decreases in the galls induced by RKN infection. This hypothesis is supported by the downregulation of the *COPT2* gene, encoding a copper importer, in the *Arabidopsis* gall transcriptome (Jammes *et al*., 2005). Micronutrients quantifications have also demonstrated a decrease in copper concentration in RKN-infected susceptible tomato roots (Lobna *et al*., 2017).

The ***SPL7*/*MIR408-UCC2*/*MIR398-CSD1* copper module** may be a key factor in gall formation, conserved across the plant kingdom. MiR408 and miR398 have been identified in more than 40 plant species (Griffiths-Jones *et al*., 2007) and *SPL7* is widely conserved throughout the plant kingdom (Yamasaki *et al*., 2009). Moreover, the targeting of *UCLACYANIN2* by miR408 and of *CSD1* by miR398 is conserved in both dicotyledonous and monocotyledonous plants (Zhang *et al*., 2017; Thatcher *et al*., 2015). miR408 and miR398 targets are associated with lignin metabolism either directly like *UCC2* (Reyt *et al*., 2020) or indirectly like *CSD1 via* the ROS. Cell wall lignin is restructured during the development of the feeding cells and galls are subject to extensive changes in vascularization, resulting in the giant cells being encaged within a network of *de novo* formed xylem and phloem cells (Bartlem, Kones and Hammes, 2014). Therefore miR398 and miR408 may be involved in modification of feeding cell wall lignin or lignin network within galls. Moreover, a role for UCLACYANINS in the formation of a lignified nanodomain within the Casparian strips known to form an endodermal barrier in *Arabidopsis* roots has recently been described (Reyt *et al*., 2020). Casparian strip defects have been observed in the endodermis bordering the giant cell area within sorghum galls induced by *M. naasi* (Ediz and Dickerson, 1976). Moreover, *Arabidopsis* mutants with disrupted Casparian strips are particularly susceptible to RKN (Holbein *et al*., 2019). The infection of plants with nematodes may, therefore, provides a unique model for investigating the role of copper modulation, *via* microRNAs and its targets, in the formation of Casparian strips.

Acknowledgements

We would like to thank Dr. Nicolas Bouché (INRAE Versailles, France) for helpful discussions and for providing the *mbcbp* and *mcsd1 Arabidopsis* lines. We would like to thank Dr. Lei Li

(Beijing University, China) for providing the *pMIR408:GUS Arabidopsis* line. We would also like to thank Dr. Toshiharu Shikanai (Kyoto University, Japan) for providing the *pSPL7:GUS* and ko *spl7 Arabidopsis* lines. The microscopy work was performed at the SPIBOC imaging facility of Institut Sophia Agrobiotech. We thank Dr Olivier Pierre and the entire team of the platform for assistance with microscopy. This work was funded by the INRAE SPE department and the French Government (National Research Agency, ANR) through the 'Investments for the Future' LabEx SIGNALIFE: programme reference #ANR-11-LABX-0028-01 and IDEX UCAJedi ANR-15-IDEX-0, and by the French-Japanese bilateral collaboration programme PHC SAKURA 2019 #43006VJ. Y.N. was supported by a doctoral fellowship from Lebanon (Municipal Council of Aazzée, Lebanon).

Author contribution

YN, S.J.P and B.F. designed the study and wrote the manuscript. Y.N., J.M. and S.J.P. designed the study and performed the experimental work. All authors analysed and discussed the data. M.Q. and P.A. participated in the writing of the manuscript. S.T. participated in the copper studies. MdR analysed NGS data. KM and YN performed the qPCR.

Data availability

The data that support the findings of this study are available from the corresponding author upon reasonable request.

References:

Abad P, Williamson VM. **2010**. Plant Nematode Interaction: A Sophisticated Dialogue. *Advances in Botanical Research* **53**: 147–192.

de Almeida Engler J, Gheysen G. **2013**. Nematode-induced endoreduplication in plant host cells: why and how? *Molecular Plant-Microbe Interactions* **26**: 17–24.

Araki R, Mermod M, Yamasaki H, Kamiya T, Fujiwara T, Shikanai T. **2018**. SPL7 locally regulates copper-homeostasis-related genes in Arabidopsis. *Journal of Plant Physiology* **224**–**225**: 137–143.

Axtell MJ. **2013**. Classification and Comparison of Small RNAs from Plants. *Annual Review of Plant Biology* **64**: 137–159.

Barciszewska-Pacak M, Milanowska K, Knop K, Bielewicz D, Nuc P, Plewka P, Pacak

AM, Vazquez F, Karlowski W, Jarmolowski A, *et al.* 2015. Arabidopsis microRNA expression regulation in a wide range of abiotic stress responses. *Frontiers in Plant Science* **6**: 410.

Bartlem DG, Jones MGK and Hammes UZ. 2013. Vascularization and nutrient delivery at root-knot nematode feeding sites in host roots. *Journal of Experimental Botany* **65**: 1789-1798.

Beauclair L, Yu A, Bouché N. 2010. MicroRNA-directed cleavage and translational repression of the copper chaperone for superoxide dismutase mRNA in Arabidopsis. *Plant Journal* **62**: 454–462.

Bernal M, Casero D, Singh V, Wilson GT, Grande A, Yang H, Dodani SC, Pellegrini M, Huijser P, Connolly EL, *et al.* 2012. Transcriptome sequencing identifies SPL7-regulated copper acquisition genes FRO4/FRO5 and the copper dependence of iron homeostasis in Arabidopsis. *Plant Cell* **24**: 738–761.

Blok VC, Jones JT, Phillips MS, Trudgill DL. 2008. Parasitism genes and host range disparities in biotrophic nematodes : the conundrum of polyphagy versus specialisation. *BioEssays* **30**: 249–259.

Brousse C, Liu Q, Beauclair L, Deremetz A, Axtell MJ, Bouché N. 2014. A non-canonical plant microRNA target site. *Nucleic Acids Research* **42**: 5270–5279.

Burkhead JL, Gogolin Reynolds KA, Abdel-Ghany SE, Cohu CM, Pilon M. 2009. Copper homeostasis. *New Phytologist* **182**: 799–816.

Cabrera J, Bustos R, Favery B, Fenoll C, Escobar C. 2014. NEMATIC: A simple and versatile tool for the insilico analysis of plant-nematode interactions. *Molecular Plant Pathology* **15**: 627–636.

Cai Q, Qiao L, Wang M, He B, Lin F-M, Palmquist J, Huang S-D, Jin H. 2018. Plants send small RNAs in extracellular vesicles to fungal pathogen to silence virulence genes. *Science* **360**: 1126–1129.

Caillaud M-C, Favery B. 2016. In Vivo Imaging of Microtubule Organization in Dividing Giant Cell. *Methods in molecular biology (Clifton, N.J.)* **1370**: 137–44.

Caillaud M-C, Lecomte P, Jammes F, Quentin M, Pagnotta S, Andrio E, de Almeida Engler J, Marfaing N, Gounon P, Abad P, *et al.* 2008. MAP65-3 microtubule-associated protein is essential for nematode-induced giant cell ontogenesis in Arabidopsis. *The Plant cell*

20: 423–37.

Chávez Montes RA, De Fátima Rosas-Cárdenas F, De Paoli E, Accerbi M, Rymarquis LA, Mahalingam G, Marsch-Martínez N, Meyers BC, Green PJ, De Folter S. **2014**. Sample sequencing of vascular plants demonstrates widespread conservation and divergence of microRNAs. *Nature Communications* **5**: 3722.

Curaba J, Singh MB, Bhalla PL. **2014**. miRNAs in the crosstalk between phytohormone signalling pathways. *Journal of experimental botany* **65**: 1425–38.

Dunker F, Trutzenberg A, Rothenpieler JS, Kuhn S, Pröls R, Schreiber T, Tissier A, Kemen A, Kemen E, Hückelhoven R, *et al.* 2020. Oomycete small RNAs bind to the plant RNA-induced silencing complex for virulence. *eLife* **9** :e56096.

Ediz SA, Dickerson OJ. **1976**. Life cycle, pathogenicity, histopathology, and host range of race 5 of the barley root-knot nematode. *Journal of Nematology* **8**: 228–231.

Escobar C, Barcala M, Cabrera J, Fenoll C. **2015**. Overview of root-knot nematodes and giant cells. *Advances in Botanical Research* **73**: 1–32.

Escobar C, Brown S, Mitchum MG. **2011**. Transcriptomic and Proteomic Analysis of the Plant Response to Nematode Infection. In: Jones J, Gheysen G, Fenoll C, eds. Genomics and Molecular Genetics of Plant-Nematode Interactions. Dordrecht: Springer Netherlands, 157–173.

Favery B, Dubreuil G, Chen M-S, Giron D, Abad P. **2020**. Gall-Inducing Parasites: Convergent and Conserved Strategies of Plant Manipulation by Insects and Nematodes. *Annual Review of Phytopathology* **58**: 1–22.

Favery B, Lecomte P, Gil N, Bechtold N, Bouchez D, Dalmasso A, Abad P. **1998**. RPE, a plant gene involved in early developmental steps of nematode feeding cells. *The EMBO journal* **17**: 6799–811.

Fu Y, Mason AS, Zhang Y, Lin B, Xiao M, Fu D, Yu H. **2019**. MicroRNA-mRNA expression profiles and their potential role in cadmium stress response in Brassica napus. *BMC Plant Biology* **19**: 570.

Griffiths-Jones S, Saini HK, van Dongen S, Enright AJ. **2007**. miRBase: tools for microRNA genomics. *Nucleic Acids Research* **36**: D154–D158.

Hoang NT, Tóth K, Stacey G. **2020**. The role of microRNAs in the legume–Rhizobium nitrogen-fixing symbiosis (R Mittler, Ed.). *Journal of Experimental Botany* **71**: 1668–1680.

Holbein J, Franke RB, Marhavý P, Fujita S, Górecka M, Sobczak M, Geldner N, Schreiber L, Grundler FMW, Siddique S. **2019**. Root endodermal barrier system contributes to defence against plant-parasitic cyst and root-knot nematodes. *Plant Journal* **100**: 221–236.

Hutvágner G, McLachlan J, Pasquinelli AE, Bálint É, Tuschl T, Zamore PD. **2001**. A cellular function for the RNA-interference enzyme dicer in the maturation of the let-7 small temporal RNA. *Science* **293:** 834-8.

Jammes F, Lecomte P, Almeida-Engler J, Bitton F, Martin-Magniette M-LL, Renou JP, Abad P, Favery B, De Almeida-Engler J, Bitton F, *et al.* 2005. Genome-wide expression profiling of the host response to root-knot nematode infection in Arabidopsisa. *The Plant Journal* **44**: 447–458.

Jaubert-Possamai S, Noureddine Y, Favery B. **2019**. MicroRNAs, New Players in the Plant–Nematode Interaction. *Frontiers in Plant Science* **10**: 1–8.

Jiang A, Guo Z, Pan J, Yang Y, Zhuang Y, Zuo D, Hao C, Gao Z, Xin P, Chu J, *et al.* 2021. The PIF1-miR408-PLANTACYANIN repression cascade regulates light-dependent seed germination. *Plant Cell* **33**: 1506–1529.

Kuo Y-W, Lin J-S, Li Y-C, Jhu M-Y, King Y-C, Jeng S-T. **2019**. MicroR408 regulates defense response upon wounding in sweet potato. *Journal of Experimental Botany* **70**: 469–483.

Lobna H, Aymen EM, Hajer R, Naima M-B, Najet H-R. **2017**. Biochemical and plant nutrient alterations induced by Meloidogyne javanica and Fusarium oxysporum f.Sp.radicis lycopersici co-infection on tomato cultivars with differing level of resistance to M. javanica. *European Journal of Plant Pathology* **148**: 463–472.

Ma C, Burd S, Lers A. **2015**. miR408 is involved in abiotic stress responses in Arabidopsis. *The Plant Journal* **84**: 169–187.

Maunoury N, Vaucheret H. **2011**. AGO1 and AGO2 Act Redundantly in miR408-Mediated Plantacyanin Regulation (M Bendahmane, Ed.). *PLoS ONE* **6**: e28729.

Medina C, da Rocha M, Magliano M, Ratpopoulo A, Revel B, Marteu N, Magnone V, Lebrigand K, Cabrera J, Barcala M, *et al.* 2017. Characterization of microRNAs from Arabidopsis galls highlights a role for miR159 in the plant response to the root-knot nematode Meloidogyne incognita. *New Phytologist* **216**: 882–896.

Reyt G, Chao Z, Flis P, Salas-González I, Castrillo G, Chao D-YY, Salt DE. **2020**.

569 Uclacyanin Proteins Are Required for Lignified Nanodomain Formation within Casparian
570 Strips. *Current Biology* **30**: 4103-4111.e6.

571 **Rodiuc N, Barlet X, Hok S, Perfus-Barbeoch L, Allasia V, Engler G, Séassau A, Marteu**
572 **N, de Almeida-Engler J, Panabières F, *et al.* 2016**. Evolutionarily distant pathogens require
573 the Arabidopsis phytosulfokine signalling pathway to establish disease. *Plant, Cell &*
574 *Environment* **39**: 1396–1407.

575 **Schulman BRM, Esquela-Kerscher A, Slack FJ**. **2005**. Reciprocal expression of lin-41 and
576 the microRNAs let-7 and mir-125 during mouse embryogenesis. *Developmental Dynamics*
577 **234:** 1046-54.

578 **Schulten A, Bytomski L, Quintana J, Bernal M, Krämer U**. **2019**. Do Arabidopsis
579 Squamosa promoter binding Protein-Like genes act together in plant acclimation to copper or
580 zinc deficiency? *Plant Direct* **3**: 590182.

581 **Sommer F, Kropat J, Malasarn D, Grossoehme NE, Chen X, Giedroc DP, Merchant SS**.
582 **2011**. The CRR1 Nutritional Copper Sensor in Chlamydomonas Contains Two Distinct
583 Metal-Responsive Domains. *The Plant Cell* **22**: 4098–4113.

584 **Thatcher SR, Burd S, Wright C, Lers A, Green PJ**. **2015**. Differential expression of
585 miRNAs and their target genes in senescing leaves and siliques: Insights from deep
586 sequencing of small RNAs and cleaved target RNAs. *Plant, Cell and Environment* **38**: 188–
587 200.

588 **Thomson JM, Newman M, Parker JS, Morin-Kensicki EM, Wright T, Hammond SM**.
589 **2006**. Extensive post-transcriptional regulation of microRNAs and its implications for cancer.
590 *Genes and Development* **20:** 2202-7.

591 **Weiberg A, Jin H**. **2015**. Small RNAs—the secret agents in the plant–pathogen interactions.
592 *Current Opinion in Plant Biology* **26**: 87–94.

593 **Weiberg A, Wang M, Lin F-M, Zhao H, Zhang Z, Kaloshian I, Huang H-D, Jin H**. **2013**.
594 Fungal Small RNAs Suppress Plant Immunity by Hijacking Host RNA Interference
595 Pathways. *Science* **342**: 118–123.

596 **Wiggers RJJ, Starr JLL, Price HJJ**. **1990**. DNA content and variation in chromosome
597 number in plant cells affected by Meloidogyne incognita and M. arenaria. *Phytopathology* **80**:
598 1391–1395.

599 **Xu W, Meng Y, Wise RP**. **2014**. Mla- and Rom1-mediated control of microRNA398 and

chloroplast copper/zinc superoxide dismutase regulates cell death in response to the barley powdery mildew fungus. *New Phytologist* **201**: 1396–1412.

Yamaguchi YL, Suzuki R, Cabrera J, Nakagami S, Sagara T, Ejima C, Sano R, Aoki Y, Olmo R, Kurata T, *et al.* 2017. Root-Knot and Cyst Nematodes Activate Procambium-Associated Genes in Arabidopsis Roots. *Frontiers in Plant Science* **8**: 1–13.

Yamasaki H, Abdel-Ghany SE, Cohu CM, Kobayashi Y, Shikanai T, Pilon M. 2007. Regulation of copper homeostasis by micro-RNA in Arabidopsis. *Journal of Biological Chemistry* **282**: 16369–16378.

Yamasaki H, Hayashi M, Fukazawa M, Kobayashi Y, Shikanai T. 2009. SQUAMOSA promoter binding protein-like7 is a central regulator for copper homeostasis in Arabidopsis. *Plant Cell* **21**: 347–361.

Zhang H, Li L. 2013. SQUAMOSA promoter binding protein-like7 regulated microRNA408 is required for vegetative development in Arabidopsis. *Plant Journal* **74**: 98–109.

Zhang J-P, Yu Y, Feng Y-Z, Zhou Y-F, Zhang F, Yang Y-W, Lei M-Q, Zhang Y-C, Chen Y-Q. 2017. MiR408 Regulates Grain Yield and Photosynthesis via a Phytocyanin Protein. *Plant Physiology* **175**: 1175–1185.

Zhang H, Zhao X, Li J, Cai H, Deng XW, Li L. 2014. Microrna408 is critical for the HY5-SPl7 gene network that mediates the coordinated response to light and copper. *Plant Cell* **26**: 4933–4953.

Zhao J, Mejias J, Quentin M, Chen Y, de Almeida-Engler J, Mao Z, Sun Q, Liu Q, Xie B, Abad P, *et al.* 2020. The root-knot nematode effector MiPDI1 targets a stress-associated protein (SAP) to establish disease in Solanaceae and Arabidopsis. *New Phytologist* **228**: 1417–1430.

Supporting Information

Fig. S1 Localisation of pMIR408 activity in fully developed galls of *Arabidopsis thaliana*.

Fig S2 Relative quantification of premiR408 and of *UCC2* and *PP2G* transcripts by qPCR in galls in comparison to uninfected *Arabidopsis thaliana* roots at 7 and 14 dpi

Fig. S3 Root phenotype of the *mir408-1* and *mir408-2 Arabidopsis thaliana* KO lines.

Fig. S4 Root phenotype of the *spl7 Arabidopsis thaliana* KO line.

Fig. S5 Relative quantification of premiR398b/c and of *CSD1, CSD2* and *BCBP* transcripts by qPCR in galls in comparison to uninfected *Arabidopsis thaliana* roots at 7 and 14 dpi.

Fig. S6. Root phenotype and area covered by the feeding site in the *mcsd1* and *mbcbp* *Arabidopsis thaliana* lines.

Fig. S7 Assessment of copper toxicity in *Meloidogyne incognita* J2s.

Fig. S8 Repression of pMIR408 activity in *Arabidopsis thaliana* galls by watering with CuSO4, assessed at 14 days post infection (dpi).

Fig. S9 Root phenotype of *Arabidopsis thaliana* Col0 watered with 50 µM copper sulphate.

Fig. S10 NBT staining of O^{2-} on 14 dpi *Arabidopsis thaliana* gall sections.

Table S1 Primers used in qPCR.

Table S2 Expression level of mature sequence of the miR408 and miR398 families upregulated in *Arabidopsis thaliana* and tomato (*Solanum lycopersum*) galls.

Table S3: Infection assays with *miR408-1* and *miR408-2 Arabidopsis thaliana* ko lines infected with *Meloidogyne incognita*.

Table S4 : Prediction of *Arabidopsis thaliana* miR408 targets with psRNA targets and expression profile of these targets in *Arabidopsis thaliana* galls.

651 **Table S5 :** Relative quantification of premiR408 and of *UCC2* and *PP2G* transcripts by
652 qPCR in galls in comparison to uninfected *Arabidopsis thaliana* roots at 7 and 14 dpi.

653 **Table S6 :** Infection assays with *spl7-1 Arabidopsis thaliana* lines infected with *Meloidogyne*
654 *incognita*.

655 **Table S7 :** Relative quantification of premiR398b/c and of *CSD1, CSD2* and *BCBP*
656 transcripts by qPCR in galls in comparison to uninfected *Arabidopsis thaliana* roots at 7 and
657 14 dpi.

658 **Table S8 :** Infection assays with *mbcbp* and *mcsd1 Arabidopsis thaliana* lines infected with
659 *Meloidogyne incognita*.

660 **Table S9 :** *Meloidogyne incognita* second stage juvenile (J2) survival after being incubated
661 for 24 hours in a CuSO4 solution.

662 **Table S10 :** Infection assays of *Meloidogyne incognita* Col0 watered with 50 µM CuSO4 or
663 tap water.

664 **Methods S1** Biological Materials, Growth Conditions

665 **Methods S2** RNA extraction

666 **Methods S3** RNA sequencing

667 **Methods S4** miRNAs Analysis

668 **Methods S5** mRNA sequencing

669 **Methods S6** mRNA Analysis

670 **Methods S7** NBT staining

671

672

673

Table & Figures

Table 1. Expression profile of miRNAs of the miR408 and miR398 families in *Arabidopsis thaliana* and tomato galls.

miRNA family	miRNA name	Plant species	miRNA mature sequence	logFC G/R 7dpi	adj. pvalue	logFC G/R 14dpi	adj. pvalue
mir408	SL3.0ch01_346	*S. lycopersicum*	TGCACAGCCTCTTCCCTGGCT	3,741	0,000	3,289	0,017
	SL3.0ch01_419	*S. lycopersicum*	TGCACTGCCTCTTCCCTGGCT	1,287	0,029	3,133	0,033
	Ath-miR408	*A. thaliana*	ATGCACTGCCTCTTCCCTGGC	2,042	0,042	2,411	0,001
mir398	SL3.0ch12_14_3	*S. lycopersicum*	ATGTGTTCTCAGGTTACCCCT	3,272	0,009	2,166	0,066
	SL3.0ch05_225	*S. lycopersicum*	TTGTGTTCTCAGGTCACCCCT	0,290	0,863	3,430	0,015
	SL3.0ch11_437	*S. lycopersicum*	TATGTTCTCAGGTCGCCCCTG	2,144	0,112	1,759	0,067
	ath-miR398b-c	*A. thaliana*	TGTGTTCTCAGGTCACCCCTT	2,464	0,119	3,287	0,000

For each miRNA family, the reference in *Arabidopsis* (Ath-miR) and in *Solanum lycopersicum* (SL3.0ch) genomes is indicated. The sequence of the mature sequence, the log2 of the Gall/uninfected root expression fold change (Log2FC G/R) and statistical significance according to the Benjamini Hochberg adjustment (adj. pvalue) for the differentially expressed miRNAs at 7 and 14 days post infection (dpi) are indicated. MicroRNAs statistically upregulated in galls in comparison to uninfected roots are underlined in red.

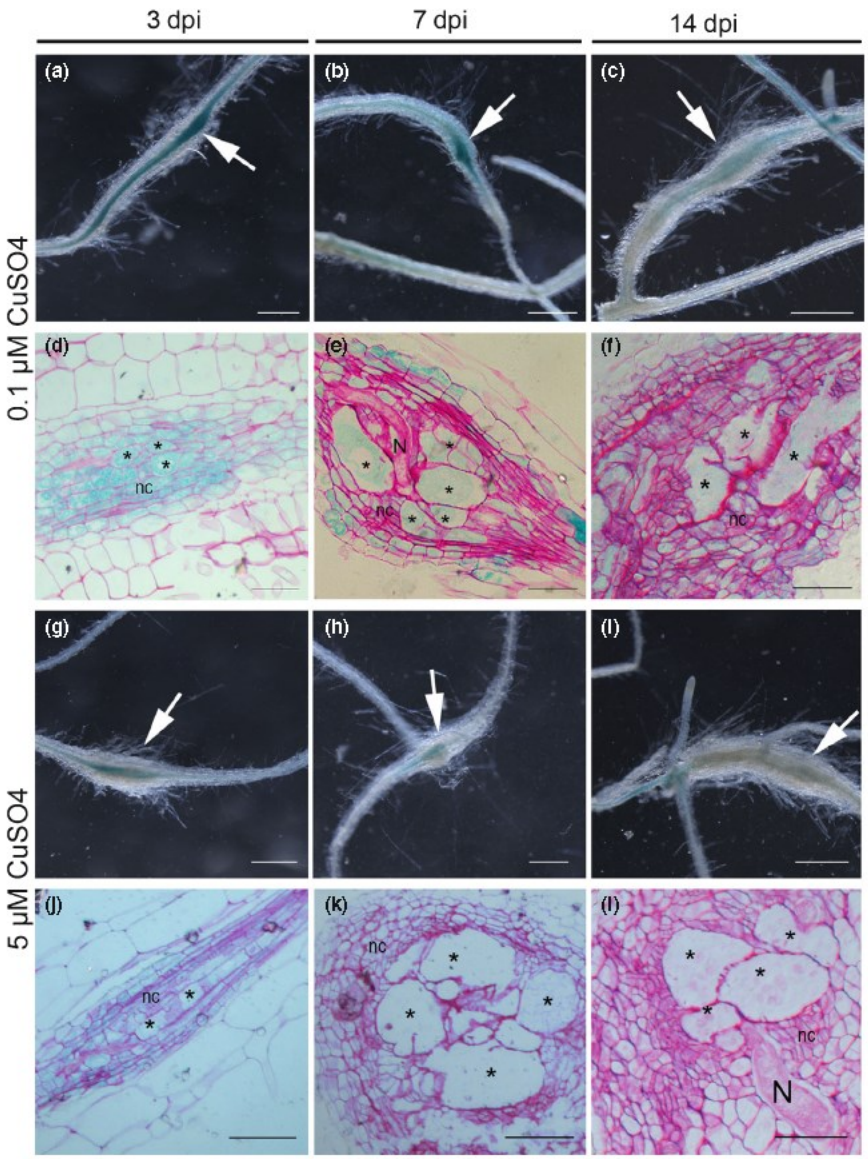

687

688 **Figure 1.** Copper modulates *MIR408* promoter activity in galls. (a-h), The activity of the
689 *MIR408* promoter was analysed in galls induced by *M. incognita* in *Arabidopsis thaliana*
690 expressing the *pMIR408*::GUS construct grown in the presence of normal concentrations of
691 copper (0.1 µM CuSO4)(a-f) or in the presence of high concentrations of copper (5.0 µM
692 CuSO4)(g-l). (a-c), a strong blue coloration reflecting GUS activity was observed in galls 3
693 days post infection (dpi) (a), 7 dpi (b) and 14 dpi (c) in plants grown with 0.1 µM CuSO4. D-
694 F, Section of galls at 3 dpi (d), 7dpi (e) and 14 dpi (f) showing the GUS blue signal in giant
695 cells and in the cells surrounding the giant cells. (g-i), a weaker GUS signal was observed in
696 galls from plants grown with 5.0 µM CuSO4 analysed at 3 dpi (g) and 7 dpi (h) and no GUS
697 signal was observed in galls at 14 dpi (i). (j-l), Section of gall at 3 dpi (j), 7dpi (k) and 14 dpi
698 (l). Galls are indicated with an arrow; N, nematode; (*) giant feeding cells; nc, neighbouring
699 cells. Bars 500 µm (a-c; g-i) or 50 µm (d-f; j-l).

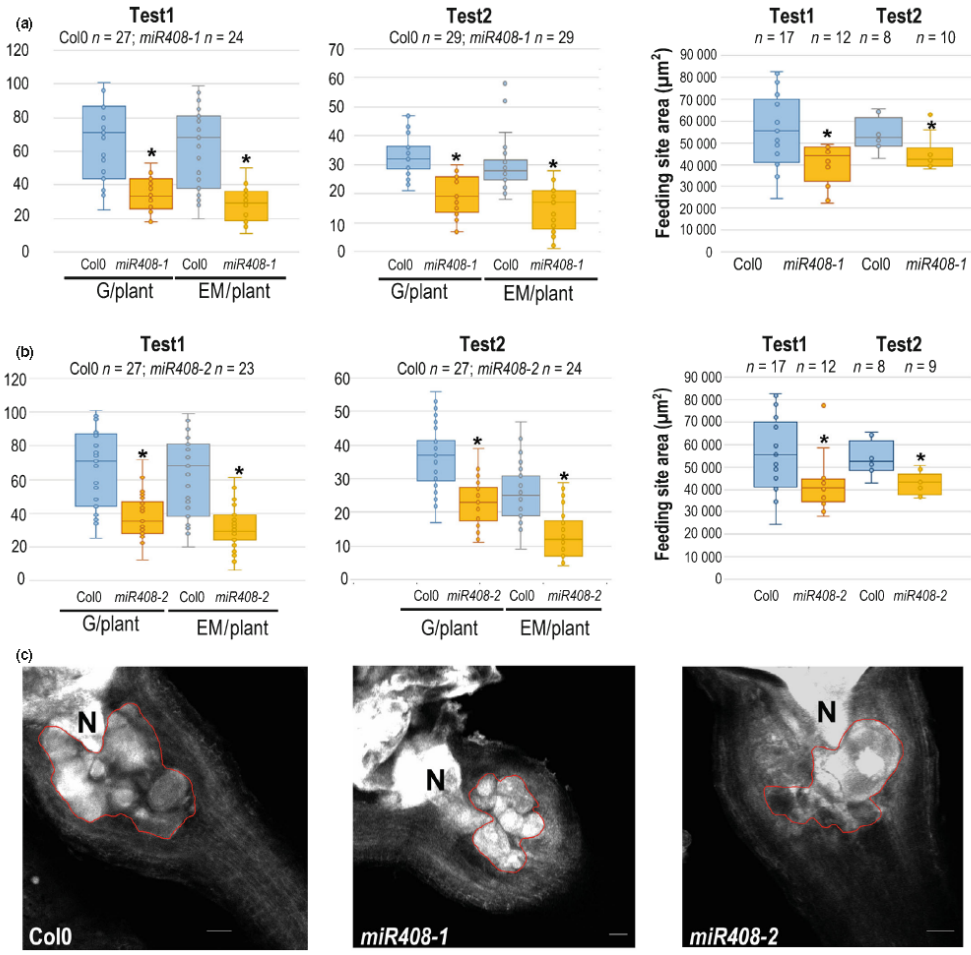

Figure 2: The *miR408* KO *Arabidopsis thaliana* lines were significantly less susceptible to *Meloidogyne incognita* than the wild type. (a-b) The susceptibility of the two *mir408* KO lines, *mir408-1* (a) & *mir408-2* (b), and Col0 wild type to *M. incognita* was evaluated by counting the number of galls and egg masses per plant (G/plant and EM/plant, respectively) in two independent infection assays in soil. (c) The effect of *MIR408* mutation on the development of giant feeding cells was further evaluated by measuring the size of the feeding site (circled in red) produced in each KO and comparing it to that in Col0. Galls were collected seven weeks post *in vitro* infection to measure the area (μm^2) covered by the giant cells by the BABB clearing method (Cabrera et al., 2018). The impact of plant genotype was analysed in Mann and Whitney tests.*, $P < 0.05$. Boxes indicate interquartile range (25th to the 75th percentile). The central lines within the boxes represent medians. Whiskers indicate the minimal and maximum of the usual values present in the data set. The circle outside the box represents outlier. n : the number of plants per line analysed in each assay for the number of galls and egg masses and the number of galls per line for each test for measurement of feeding site area. Bars 50µm. N : nematode.

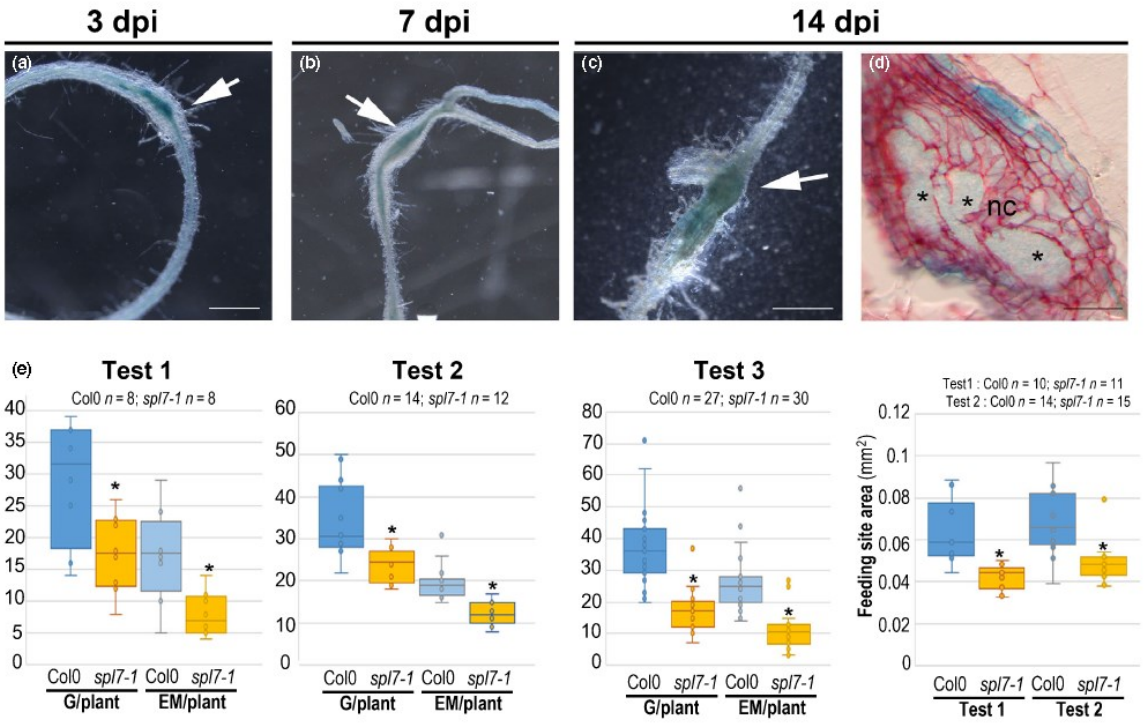

Figure 3. *SPL7* is induced and required for *Meloidogyne incognita* infection and giant cell formation in *Arabidopsis thaliana*. (a-d), The activity of the *SPL7* promoter (*pSPL7*) was studied in galls induced by *M. incognita* from *A. thaliana* expressing the *pSPL7::GUS* construct, at 3 days post inoculation (dpi)(a), 7 dpi (b) and 14 dpi (c). (d), GUS blue staining was observed within 5.0 µm-thick gall sections at 14 dpi. (e), the KO *spl7* line (SALK093849c) was infected with M. incognita J2. This line was significantly less susceptible to RKN than Col0, as shown by the smaller mean number of galls and egg masses per plant (G/plant and EM/plant, respectively) in three independent infection assays. The effect of *spl7* mutation on the development of feeding cells was further evaluated by measuring the size of the feeding site area. Galls were collected seven weeks post *in vitro* infection for measurement of the area (mm^2) covered by the giant cells, by the BABB clearing method (Cabrera et al., 2018). Mann–Whitney tests were performed for statistical analysis in each experiment; significant differences relative to Col-0: *, $P < 0.05$. Boxes indicate interquartile range (25th to the 75th percentile). The central lines within the boxes represent medians. Whiskers indicate the minimal and maximum of the usual values present in the data set. The circle outside the box represents outlier. n : the number of plants per line analysed in each assay for the number of galls and egg masses and the number of galls per line for each test for measurement of feeding site area. Galls are indicated with an arrow; (*) giant feeding cells; nc, neighbouring cells. Bars 50 µm (a-c) or 500 µm (d).

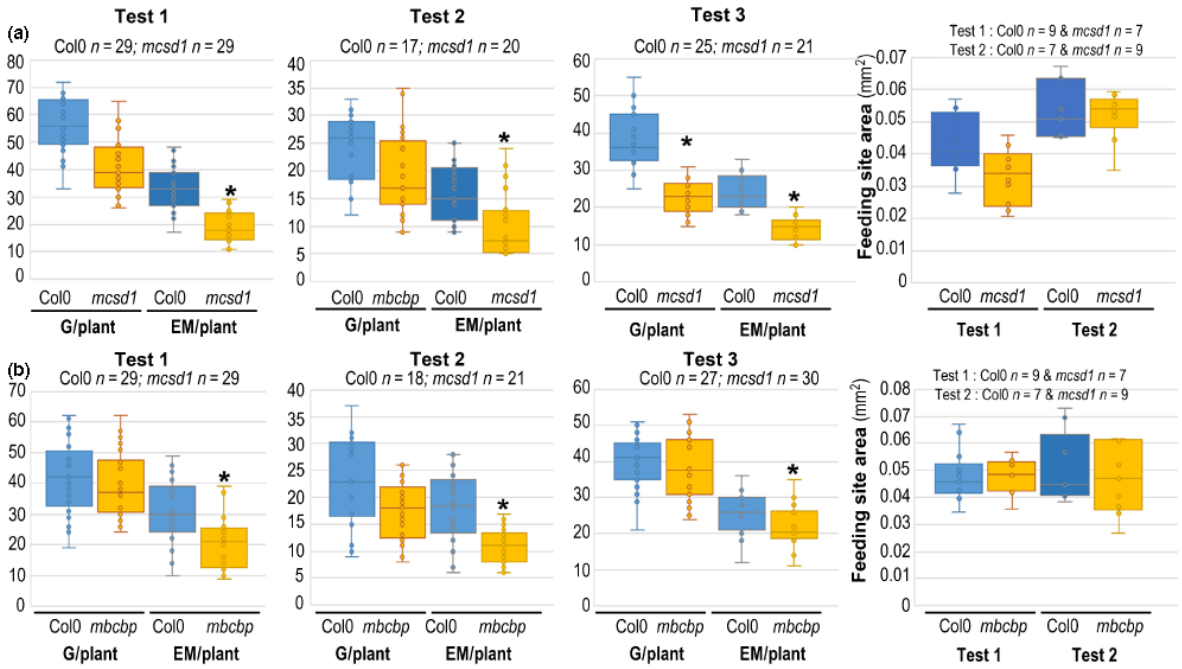

Figure 4. The miR398-resistant *mcsd1* and *mbcbp* mutant *Arabidopsis thaliana* lines had smaller numbers of egg masses. The susceptibility of the (a) *mcsd1* and (b) *mbcbp* lines and of wild-type Col0 plants was evaluated by counting the number of galls and egg masses per plant (G/plant and EM/plant, respectively) in three independent infection assays in soil. Nematode feeding site area (in mm^2) in wild-type Col0 and *mcsd1* or *mbcbp* mutants were then measured following gall clearing with BABB (Cabrera et al., 2018). Results from two independent experiments are shown. All data were analysed in Mann and Whitney statistical tests.*, $P < 0.05$. Boxes indicate interquartile range (25th to the 75th percentile). The central lines within the boxes represent medians. Whiskers indicate the minimal and maximum of the usual values present in the data set. The circle outside the box represents outlier. n : the number of plants per line analysed in each assay for the number of galls and egg masses and the number of galls per line for each test for measurement of feeding site area.

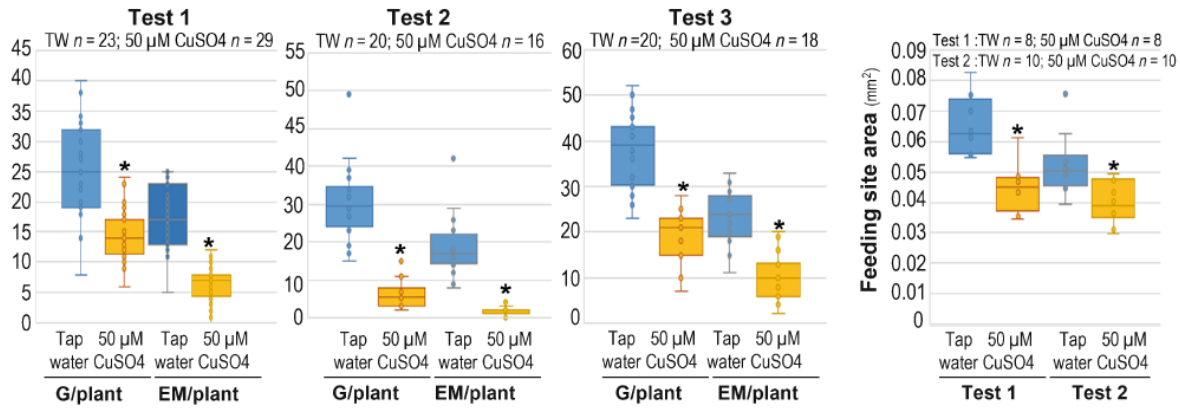

Figure 5. ***Arabidopsis thaliana*** **Col0 watered with copper sulphate solution were significantly less susceptible**

to root-knot nematodes. The effect of physiological concentrations of copper on *Meloidogyne incognita* infection was evaluated by counting galls and egg masses per plant (G/plant and EM/plant, respectively) in Col0 plants watered with tap water (TW) or with a copper sulphate ($CuSO_4$) solution at a non-toxic concentration (50 µM) Three independent experiments were performed. Nematode feeding site area (in mm^2) in wild-type Col0 cultivated on tap water or on 50 µM $CuSO^4$ were then measured following gall clearing with BABB (Cabrera et al., 2018). Results from two independent experiments are shown. All data were analysed in Mann and Whitney statistical tests.*, $P < 0.05$. Boxes indicate interquartile range (25th to the 75th percentile). The central lines within the boxes represent medians. Whiskers indicate the minimal and maximum of the usual values present in the data set. The circle outside the box represents outlier. n : the number of plants per line analysed in each assay for the number of galls and egg masses and the number of galls per line in each test for measurement of feeding site area.